

ICONE  
Conference Paper

American Society of Mechanical Engineers (ASME) owns all copyright and publication subject to this requirement: "Verbatim reproduction of this paper by anyone will be permitted by ASME provided appropriate credit is given to the author(s) and ASME."

ICONE10-22381

**DIRECT CONTACT HEAT EXCHANGE INTERFACIAL PHENOMENA FOR LIQUID  
 METAL REACTORS: PART I-HEAT TRANSFER**

D. H. Cho, R. J. Page, D. Hurtault\*  
 Argonne National Laboratory  
 Reactor Analysis and Engineering Division  
 9700 South Cass Avenue  
 Argonne, Illinois 60439, USA  
 (\*Intern from INSTN, CEA/Saclay, France)

S. Abdulla, X. Liu, M. H. Anderson, R. Bonazza,  
 M. L. Corradini  
 University of Wisconsin-Madison  
 Wisconsin Institute of Nuclear Systems  
 Engineering Physics  
 Madison, Wisconsin 53706, USA

**ABSTRACT**

Experiments on direct-contact heat exchange between molten metal and water for steam production were conducted. These experiments involved the injection of water into molten lead-bismuth eutectic for heat transfer measurements in a 1-D geometry. Based on the initial results of the experiments, the effects of the water flow rate and the molten metal superheat (temperature difference between molten metal and saturated water) on the volumetric heat transfer coefficient were discussed.

**KEYWORDS:** advanced reactors, molten metal, direct-contact heat exchange

**INTRODUCTION**

An innovative design concept for liquid-metal cooled reactors involves direct-contact heat exchange between molten metal and water for steam production (Buongiorno et al., 2000; Kinoshita et al., 2000). While the concept offers a potential for cost reduction, it presents a number of technically challenging issues, most of which are related to the interfacial transport phenomena and associated hydrodynamic stability in the molten metal-water mixture. To aid in addressing these issues, experiments involving the injection of water into molten metal are being conducted at Argonne National Laboratory (ANL) and the University of Wisconsin - Madison (UW). The ANL experiments are primarily concerned with global heat transfer measurements including the volumetric heat transfer coefficient in a 1-D geometry, while the UW experiments focus on local measurements including the X-ray imaging of the melt/water/steam mixture in a 2-D geometry. The initial results of the ANL experiments are described in this paper. The UW work will be presented in a companion paper (Abdulla et al., 2002).

**NOMENCLATURE**

$C_p$	=	specific heat of water
$h_{fg}$	=	heat of vaporization of water
$\dot{m}_c, \dot{m}_d, \dot{m}_w$	=	mass flow rates of continuous phase, dispersed phase and water, respectively
$U_v$	=	volumetric heat transfer coefficient
$V$	=	volume of molten metal-water mixing zone
$Z$	=	height of molten metal-water mixing zone
$Z_o$	=	collapsed height of molten metal only
$\alpha$	=	void fraction of molten metal-water/steam mixture
$\Delta T$	=	temperature difference between molten metal and saturated water
$\Delta T_{sub}$	=	water subcooling

**KEY PARAMETERS AND EXPERIMENTAL NEEDS**

Over the years, a number of experiments have been conducted to provide measurements on direct contact heat transfer and evaporation of cold, volatile liquid drops dispersed in the continuous phase of hot liquid, as have been reviewed by Kim et al. (2000). This review suggests that the following four parameters play a key role in determining the heat transfer characteristics.

- 1) Dispersed phase mass-flux ( $\dot{m}_d$ )

For low values of  $\dot{m}_d$ , the volumetric heat transfer coefficient increases with increasing  $\dot{m}_d$ . However, it

reaches a maximum and then decreases moderately for higher values of  $\dot{m}_a$ . This behavior appears to be related to a flow regime transition from bubbly to churn turbulent.

2) Continuous phase mass flux ( $\dot{m}_c$ )

For counter current flows (i.e.,  $\dot{m}_a$  and  $\dot{m}_c$  are in opposite directions), the volumetric heat transfer coefficient appears to increase with increasing value of  $\dot{m}_c$  for a given  $\dot{m}_a$ . It is not clear whether a similar behavior would occur for co-current flows. No data exists for co-current flows, which would be of interest for reactor application.

3) Temperature difference between the hot continuous phase and the evaporating dispersed phase (i.e., boiling point) ( $\Delta T$ )

Limited data for the water/pentane pair seems to suggest that the volumetric heat transfer coefficient decreases with increasing temperature driving force,  $\Delta T$ . This effect of  $\Delta T$  may be related to the possibility of the wetted area for effective heat transfer decreasing with increasing superheat.

4) System pressure (P)

Limited data for the Woods metal/water system seems to indicate that the volumetric heat transfer coefficient decreases with increasing system pressure. This effect of the system pressure may be related to the possibility of the pressure influencing the boiling behavior of the dispersed phase and hence, the drop sizes of the dispersed phase. Recently, however, Buongiorno et al. (2001) has suggested that the observed effect of pressure on the volumetric heat transfer coefficient would be limited to bubbly flow and that in churn flow, the volumetric heat transfer coefficient could increase with increasing pressure.

The parameters discussed above are all considered important for application to an innovative reactor system involving direct contact heat transfer. Presently, however, applicable data does not exist. Consider the Pb-Bi/water direct contact reactor concept discussed by Buongiorno et al. (2000). In this reactor concept, liquid water is injected into a pool of molten lead-bismuth alloy located above the reactor core to produce superheated steam. Direct contact heat exchange conditions typically are:

1)  $\dot{m}_a = 79.4 \text{ kg/m}^2 \cdot \text{s}$ , 2)  $\dot{m}_c = 4446.0 \text{ kg/m}^2 \cdot \text{s}$  (co-current),

3)  $T = 210^\circ\text{C}$  and 4)  $P = 7.0 \text{ MPa}$ . The only available data for liquid metal/water direct contact heat transfer were obtained at CRIEPI in Japan (Kinoshita et al., 1995, 1997, 2000). Test conditions for these data were 1)  $\dot{m}_a = 0.028 - 0.074 \text{ kg/m}^2 \cdot \text{s}$ ,

2)  $\dot{m}_c =$  essentially zero, 3)  $\Delta T = 20 - 50^\circ\text{C}$  and

4)  $P = 0.1 - 1.0 \text{ MPa}$ . Clearly, the CRIEPI data is very limited. In particular, the dispersed phase mass fluxes for the CRIEPI data

represent only one thousandth of the value being considered for the proposed reactor concept of Buongiorno et al. (2000). In addition, no data is available for significant co-current flows at all. Thus, experiments covering wider ranges of the four parameters discussed above are clearly needed. This paper presents the initial results of experiments looking at the effects of two parameters, namely  $\dot{m}_a$  and  $\Delta T$ .

## EXPERIMENTAL APPARATUS AND PROCEDURE

Experimental Apparatus: The experimental apparatus is shown schematically in Fig. 1. It consists of a test section and associated components (e.g., water supply tank, condenser, melt vessel, containment vessel, and instrumentation).

The test section is a 1.0-m long section of a 0.095-m I.D., 0.0095-m thick Type 410 SS seamless pipe. It is instrumented with 39 thermocouples equi-spaced along its length and protruding through the wall on the inside. In addition, there are 8 thermocouples secured to the outer wall of the test section, two at each of four axial locations. There is also a pressure transducer located at the top of the test section. The test section is heated by high-power density band heaters clamped around the outside wall. The water injection port is inserted into the test section through the base of the test section. The basic design of the injector is a stainless steel tube with a single hole at the exit. The injector hole size was 2 mm in diameter for the first test (NERI-4) and 1 mm in diameter for later tests (NERI-5 and NERI-6). The top of the test section is closed except for a 0.0127-m OD tube that carries steam through the top of the containment vessel to a condenser system.

The melt vessel is a 0.5-m long section of a Schedule 40, 4-inch SS pipe heated by band heaters. It is located next to the test section. The test section and melt vessel are joined by a 0.00635-m OD stainless steel tube through which molten metal is transferred. During runs when water is injected into molten metal, the test section and melt vessel are placed in a containment chamber. The body of the containment chamber is a 1.8-m long section of a 0.91-m O.D., 0.025-m thick carbon steel pipe. The containment chamber provides blast protection from potential explosive interactions between molten metal and water and also environmental protection from lead alloy contamination.

Water is pumped from a supply tank to the injector through a set of filters. The water flowrate is metered by valves and measured by flowmeters with ranges of 14 to 100 ml/min and 50 to 500 ml/min. There is also an argon supply to the injector, the purpose being to have flow through the injector while molten metal is being transferred to the test section from the melt vessel. Without this argon flow, metal would flow down into the injector and plug it.

When metal has been transferred from the melt vessel to the test section, an air supply into the containment vessel is turned on to freeze metal in the transfer tube and prevent inadvertent transfer back to the melt vessel.

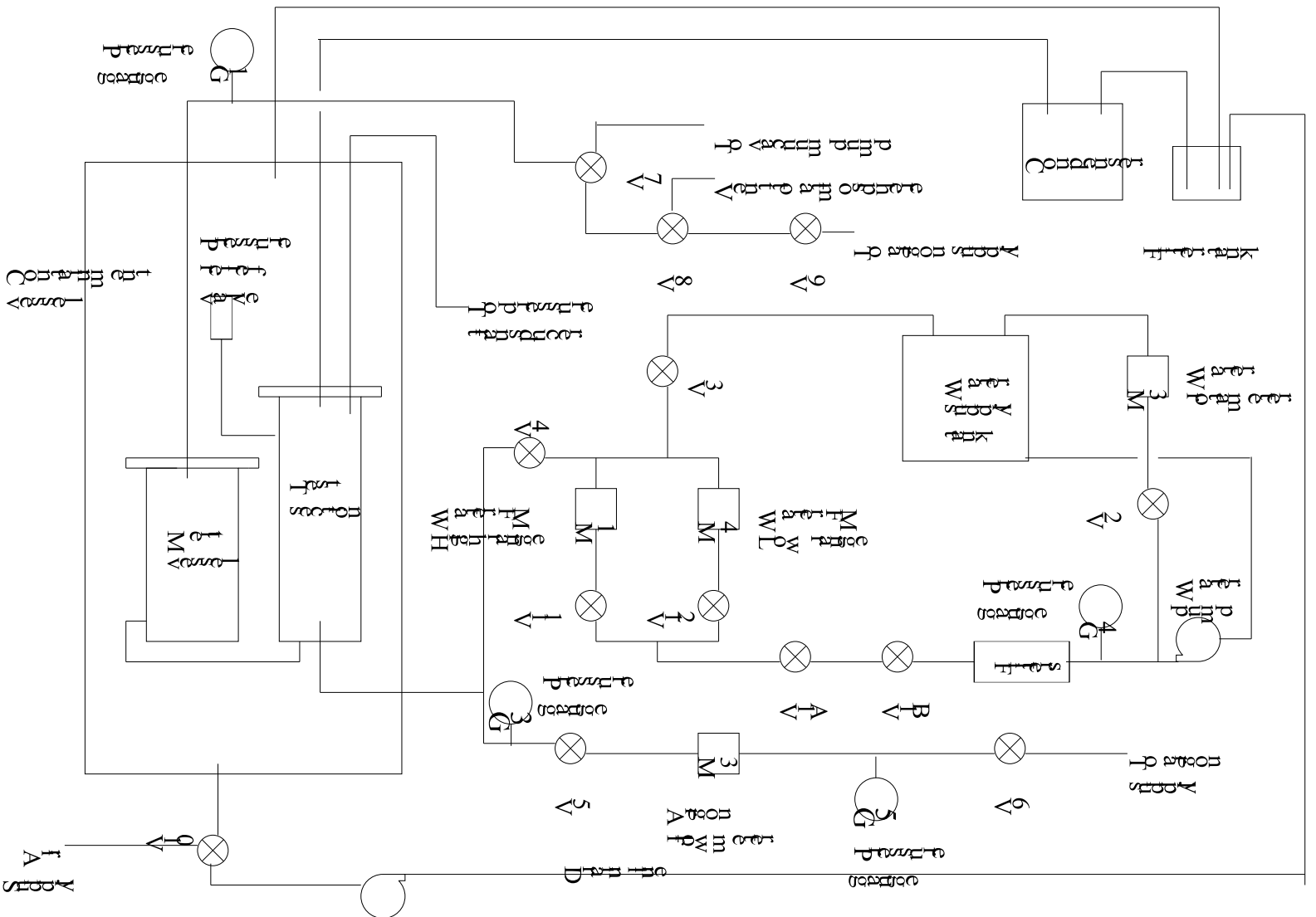


Figure 1: Schematic of the power system

Finally, a pump is provided that would remove any water that condensed inside the containment vessel. However, this should not happen since the steam is exhausted into a condenser outside of the containment vessel.

**Test Procedure:** Lead alloy (lead-bismuth eutectic, m.p. = 125°C) that has previously been loaded into the melt vessel is heated to a temperature sufficiently above the melting point for the lead alloy to flow easily. Once this temperature is reached, lead alloy starts to flow under gravity from the melt vessel into the test section. To complete the transfer, the melt vessel is pressurized with argon. During the transfer, a flow of argon gas through the injector is maintained to prevent backflow of molten metal into the injection port. Once transfer is complete, as indicated by level probes in the test section, the air supply to the containment vessel is turned on and the heater on the transfer tube is turned off. This enables a metal plug to form and prevents molten lead alloy from flowing back into the melt vessel. The molten metal in the test section may now be further heated. When the desired metal temperature is reached, water flow to the injector is turned on at a pre-set rate so that there is a mix of argon and water flowing through the injector. Once water flow is established, the argon flow is gradually reduced to zero. Heat transfer measurements are made using the thermocouples in the molten metal, and by measuring the power output of the test section heaters.

## RESULTS AND DISCUSSION

A total of six tests including shakedown were conducted. A major operational problem was found to be the plugging of the injection nozzle due to the backflow and freezing of the molten metal in the injector. Three successful tests with water injection were conducted. The water injection was mixed with an argon flow to minimize the plugging problem. Due to a variety of operational difficulties, sustaining steady states were not achieved in these tests. Instead, a run typically consisted of transient cooldown of the molten metal with intermittent, short-duration quasi steady states.

Data for three selected quasi steady states will be used to estimate the volumetric heat transfer coefficient. These data are presented in Figs. 2, 3 and 4, which show axial temperature profiles through the liquid metal in the test section. It is seen that the molten metal temperature is remarkably uniform and constant throughout the liquid metal-water mixing zone. We believe that the molten metal surface corresponds to the height at which the temperatures deviated significantly from the uniform distribution.

Based on the above observation of the data, the volumetric heat transfer coefficient for the molten metal-water mixture,  $U_v$ , was estimated from the expression

$$U_v = \frac{\dot{m}_w (C_p \Delta T_{sub} + h_{fg})}{V \Delta T} \quad (1)$$

where  $\dot{m}_w$  is the water injection rate,  $\Delta T_{sub}$  is the degree of subcooling of the injected water,  $C_p$  and  $h_{fg}$  are the specific heat and heat of vaporization of water, respectively,  $V$  is the volume of the molten metal-water mixture, and  $\Delta T$  is the temperature difference between the molten metal and saturated water. Eq. (1) does not include possible superheating of the steam produced, so it is considered to give a lower estimate of the volumetric heat transfer coefficient. The estimates of  $U_v$  along with the test conditions for the three quasi steady states selected are summarized in Table 1. The average void fraction of the molten metal-water/steam mixture,  $\alpha$ , was estimated by

$$\alpha = \frac{z - z_0}{z} \quad (2)$$

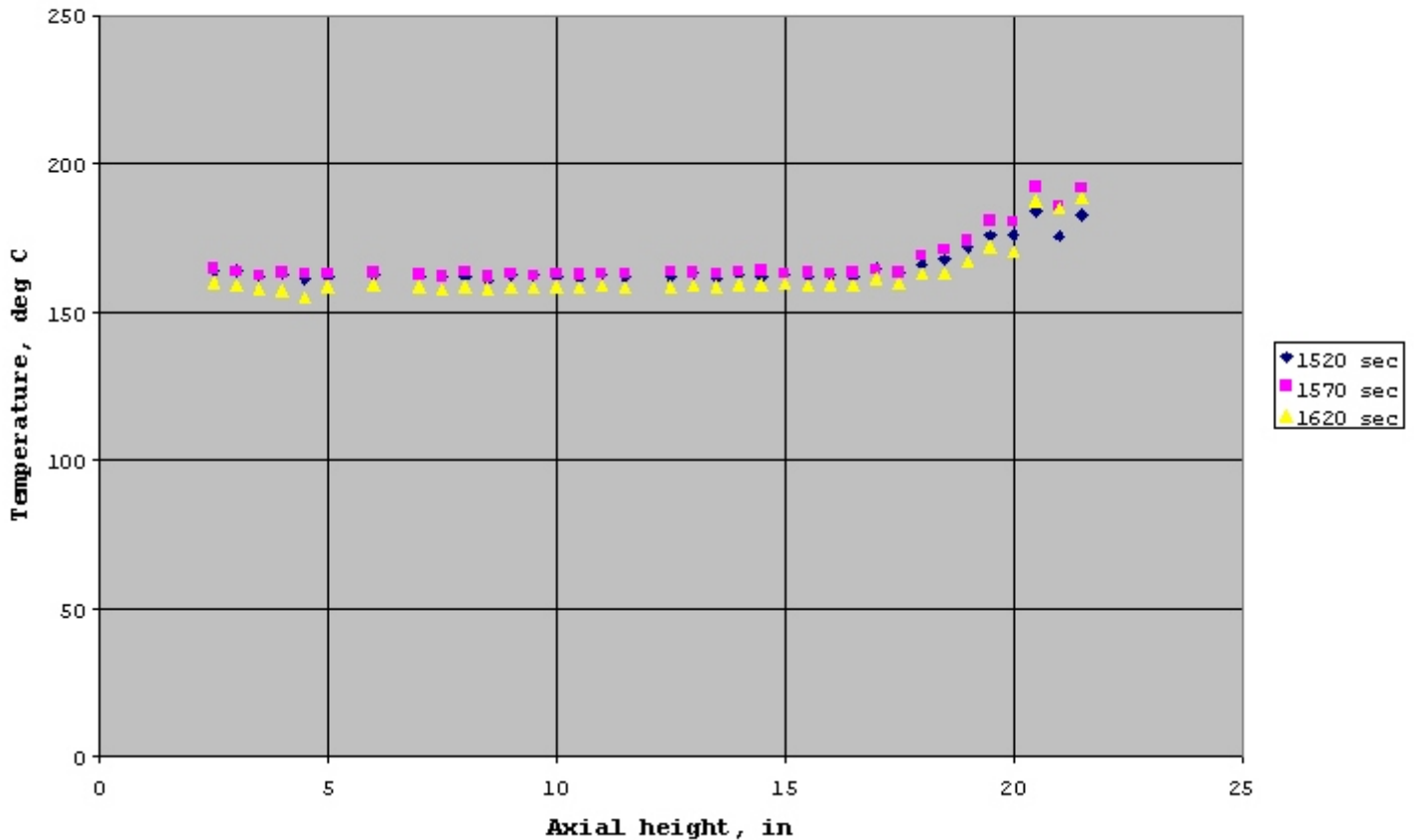
where  $z$  is the height of the molten metal-water mixing zone and  $z_0$  the collapsed height (i.e., metal only), both being measured from the water injection point.

**Table 1. Quasi Steady State Data**

Test No.	Duration	Argon Flow	Water Flow		Molten Metal Temp.	Void Fraction	Volumetric Heat Transfer Coefficient
	Sec		slpm	ml/min			mm/s*
NERI-4	100	12.7	92	0.22	160	0.28	23.2
NERI-5	85	14.4	70	0.16	175	0.35	14.1
NERI-6	400	zero	30	0.07	250	not available	4.7

\*Superficial water velocity = Total water flow rate/cross-sectional area of test section.

**Figure 2 Axial temperature profiles for NERI-4**



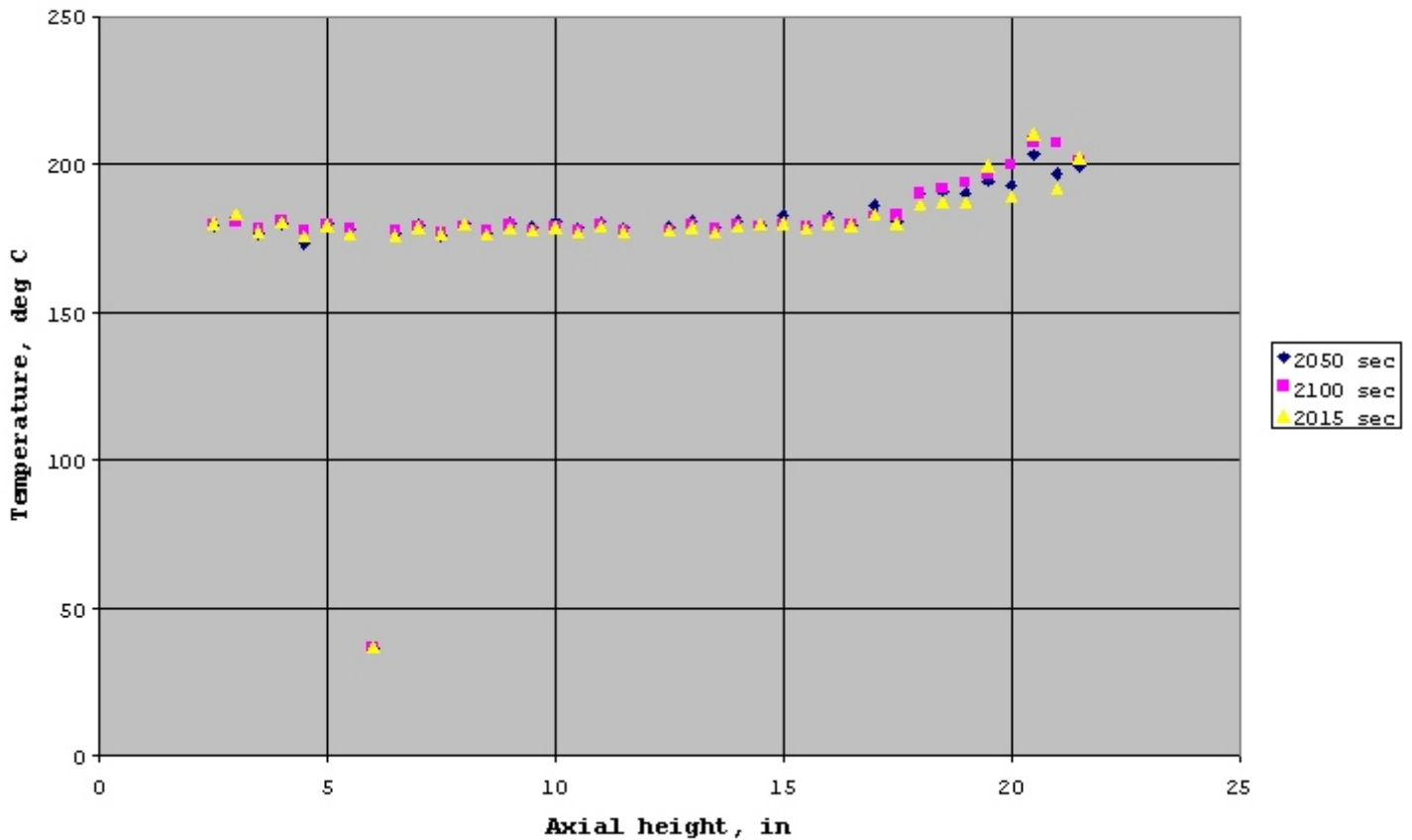
We now compare our estimates of  $U_v$  with the CRIEPI results, which appear to be the only data available for a molten metal-water system. For the CRIEPI experiment, the superficial water velocity varied from 0.028 to 0.074 mm/s and  $\Delta T$  mostly ranged from 20 to 50°C. The CRIEPI investigators reported two different volumetric heat transfer coefficients, one for the entire molten metal-water mixing zone and another for the evaporation zone. The volumetric heat transfer coefficient for the entire mixing zone was in the range of 5 to 30  $\text{KW/m}^3\text{-s}$  (Kinoshita et al., 1995) while that for the evaporation zone ranged from 30 to 50  $\text{KW/m}^3\text{-s}$  (Kinoshita et al., 1997). It thus appears that the  $U_v$  values given in Table 1 are comparable to the CRIEPI values for the entire molten metal-water mixing zone. However, the following two observations need to be made.

1) The superficial water velocities for NERI-4 and NERI-5 were significantly (several times) greater than those for the CRIEPI experiment. It is believed that in NERI-4 and NERI-5, the

steam flow in the mixing zone was in the churn turbulent regime whereas in the CRIEPI experiment, it was mostly in the bubbly regime. Thus it may not be entirely appropriate to compare the NERI-4 and NERI-5 data with the CRIEPI data. It should be noted, however, that despite the significantly larger mass fluxes of water, the  $U_v$  values estimated from NERI-4 and NERI-5 were, by and large, somewhat lower than the CRIEPI results.

2) For NERI-6, the superficial water velocity was quite comparable to those for the CRIEPI experiment and the steam flow regime was believed to be mostly bubbly. It appears that at the superficial water velocity of NERI-6 (i.e., 0.07 mm/s), the CRIEPI experiment yielded a volumetric heat transfer coefficient significantly greater than the NERI-6 estimate given in Table 1. (The CRIEPI papers do not present the volumetric heat transfer coefficient as a function of the mass flow rate of water, so it was not possible to find

Figure 3 Axial temperature profiles for NERI-5



the CRIEPI value of  $U_v$  for the NERI-6 water flow rate. However, it is believed that the value was near the upper, rather than the lower, end of the 5 - 30  $\text{KW}/\text{m}^3\text{-s}$  range mentioned earlier.) The low value of  $U_v$  for NERI-6, as compared to the CRIEPI values, may be indicative of the effect of the molten metal temperature. For NERI-6,  $\Delta T$  (temperature difference between the molten metal and saturated water, i.e., molten metal superheat) was  $150^\circ\text{C}$  whereas it was in the range of 20 to  $50^\circ\text{C}$  for the CRIEPI experiment.

#### CONCLUDING REMARKS

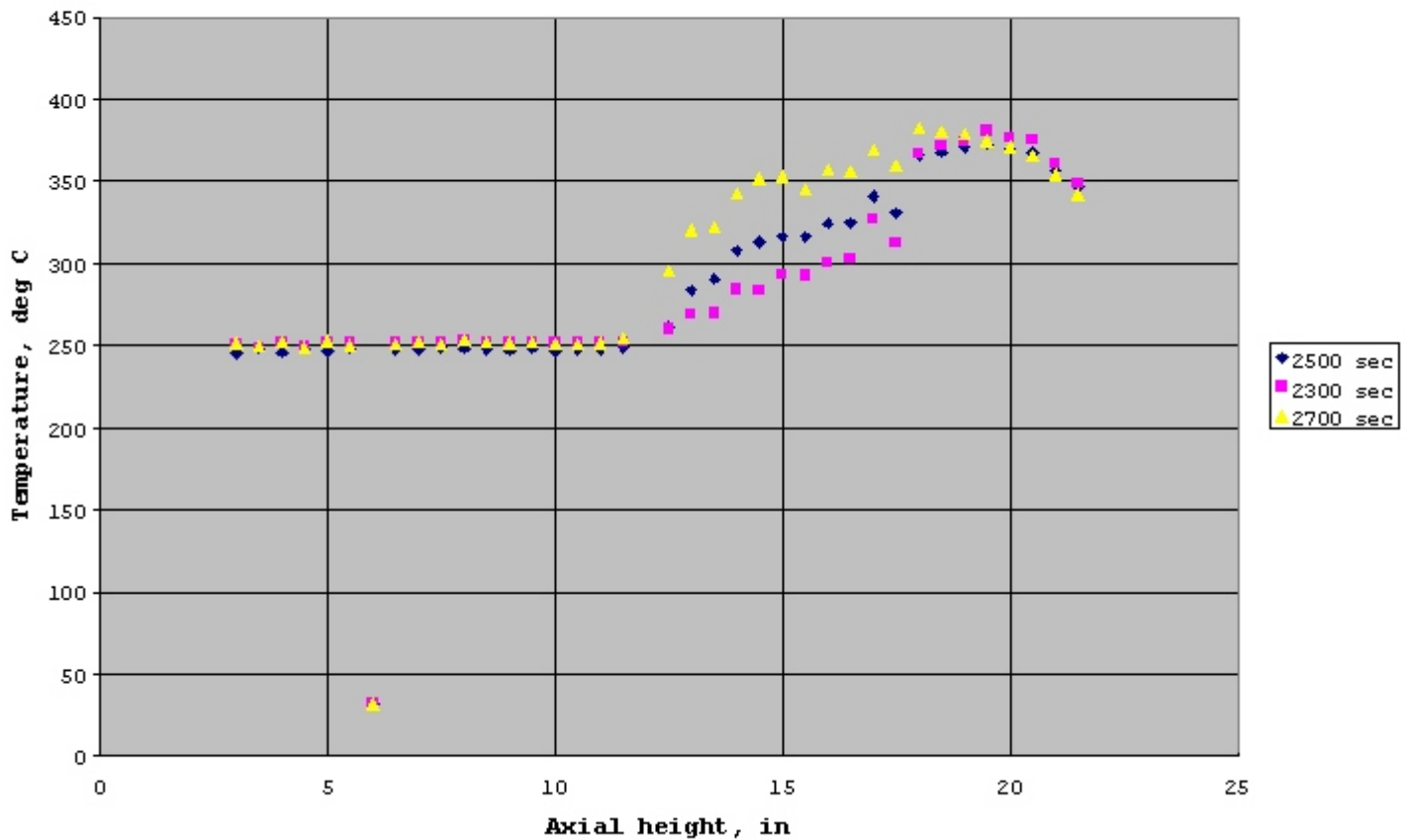
Because the data presented in this paper are very limited, it would be presumptuous to attempt to discern trends with respect to the parameters involved. However, it appears that the

volumetric heat transfer coefficient increases with increasing rate of water injection. Also, a comparison of our estimates of the volumetric heat transfer coefficient with the CRIEPI results seems to suggest that the heat transfer may become less efficient with increasing superheat of molten metal,  $\Delta T$ . The effect of  $\Delta T$  on the heat transfer rate would be expected to depend on the system pressure, as it is related to the characteristics of boiling. Experiments to obtain data at elevated pressures are underway at UW as well as ANL.

#### REFERENCES

Abdulla, S., Liu, X., Anderson, M. H., Bonazza, R., Corradini, M. L., Cho, D. H., Page, R. J., Hurtault, D., 2002, "Direct Contact Heat Exchange Interfacial Phenomena for Liquid Metal Reactors: Part II-Void Fraction," ICONE10.

**Figure 4 Axial temperature profiles for NERI-6**



Buongiorno, J., Todreas, N. E. and Kazimi, M. S., "Void Fraction Prediction for the Pb-Bi/Water Direct Contact Nuclear Reactor." Presented at the 8<sup>th</sup> International Conference on Nuclear Engineering, April 2-6, 2000, Baltimore, MD, USA, paper No. ICONE-8739.

Buongiorno, J., Todreas, N. E. and Kazimi, M. S., "Thermal Design of a Lead-Bismuth Cooled Fast Reactor with In-Vessel Direct-Contact Steam Generation." Presented at the 9<sup>th</sup> International Conference on Nuclear Engineering, April 8-12, 2001, Nice, France, paper No. ICONE-9772.

Kim, H., Anderson, M., Bonazza, R., Corradini, M. and Cho, D. H., "Interfacial Transport Phenomena and Stability in Molten Metal-Water Systems," *ibid.*, paper No. ICONE-8478.

Kinoshita, I., Nishi, Y. and Furuya, M., 1995, "Fundamental Heat Transfer Characteristics of a Direct Contact Steam Generator for Fast Breeder Reactors," Proceedings of the 3<sup>rd</sup> JSME/ASME Joint International Conference on Nuclear Engineering, Vol. 1, p. 11.

Kinoshita, I., Nishi, Y. and Furuya M., 1997, "Fundamental Heat Transfer Characteristics of Direct Contact Heat Exchanger Between Melting Alloy and Water," Experimental Heat Transfer, Fluid Mechanics and Thermodynamics 1997, M. Giot, F. Mayinger, G. P. Celata (Editors), Edizioni ETS, pp. 2071-2077.

Kinoshita, I., Nishi, Y. and Furuya, M., "Study on Applicability of Direct Contact Heat Transfer Steam Generators for LMFBRs." Presented at the 8<sup>th</sup> International Conference on Nuclear Engineering, April 2-6, 2000, Baltimore, MD, USA, paper No. ICONE-8769.